Treatment Analogous to Seasonal Change Demonstrates the Integration of Cold Responses in *Brachypodium distachyon*[1][OPEN]

Boris F. Mayer,[a] Annick Bertrand,[b] and Jean-Benoit Charron[a,2,3]

[a]McGill University, Department of Plant Science, 21,111 Lakeshore, Sainte-Anne-de-Bellevue, Quebec H9X 3V9, Canada

[b]Agriculture and Agri-food Canada, Québec Research and Development Centre, 2560 Hochelaga Boulevard, Quebec G1V 2J3, Canada

ORCID ID: 0000-0001-8547-7323 (J.-B.C.).

Anthropogenic climate change precipitates the need to understand plant adaptation. Crucial in temperate climates, adaptation to winter is characterized by cold acclimation and vernalization, which respectively lead to freezing tolerance and flowering competence. However, the progression of these responses during fall and their interaction with plant development are not completely understood. By identifying key seasonal cues found in the native range of the cereal model *Brachypodium distachyon*, we designed a diurnal-freezing treatment (DF) that emulates summer-to-winter change. DF induced unique cold acclimation and vernalization responses characterized by low *VERNALIZATION1* (*VRN1*) expression. Flowering under DF is characterized by an up-regulation of *FLOWERING LOCUS T* (*FT*) postvernalization independent of *VRN1* expression. DF, while conferring flowering competence, favors a high tolerance to freezing and the development of a winter-hardy plant structure. The findings of this study highlight the contribution of phenotypic plasticity to freezing tolerance and demonstrate the integration of key morphological, physiological, and molecular responses in cold adaptation. The results suggest a fundamental role for *VRN1* in regulating cold acclimation, vernalization, and morphological development in *B. distachyon*. This study also establishes the usefulness of reproducing natural cues in laboratory settings.

The unpredictable effects of climate change have imposed challenges to natural ecosystems and agriculture. The detrimental effects of environmental stresses on food production will become more problematic in the future (USGCRP, 2017). Unfortunately, the limited understanding of plants' adaptive mechanisms to changing environments restrains our ability to predict and prepare for these consequences. Plant adaptation is a complex concept that transcends stress responses, plant development, behavior, and evolution. Undertaking research on this topic requires a global perspective on how plants respond to change. Temperate plants have evolved to persist under seasonal climates, and their adaptation to cold and freezing is a useful system for adaptation studies. However, there are still gaps in the integrative understanding of cold adaptation, possibly due to the disparity between controlled and natural environments (Gusta and Wisniewski, 2013). Indeed, cold is a major stressor in temperate regions, and climatic events, such as late frost, will be increasingly problematic in the future. Hence, understanding the mechanisms behind plant adaptation to cold is crucial for the development of hardier plants.

Freezing tolerance is an important adaptive trait in temperate plants (Chouard, 1960). Winter-hardy plants innately possess or can acquire the structure and physiology to grow under cold and survive freezing (Thomashow, 1999; Körner, 2016). In fact, it was proposed that plant cold-adaptive characteristics can be divided into three groups: (1) genotypic traits (irreversible within one plant's lifetime), (2) modification of plant structure (in response to the environment), and (3) acclimation or physiological adjustments (that are reversible; Körner, 2016). The latter group, also called cold acclimation, has been the subject of substantial research in plants. Cold acclimation is often accompanied by the production of osmolites, cryoprotective molecules, ice formation inhibitors, and metabolic shifts that increase tolerance to freezing and the plant's

[1]This work was supported by the Natural Sciences and Engineering Research Council of Canada (NSERC Discovery grant RGPIN-2015-06679 to J.B.C.). B.F.M. was supported by the Vanier Canada Graduate Scholarship. The authors also acknowledge support from Centre SEVE.

[2]Author for contact: jean-benoit.charron@mcgill.ca.

[3]Senior author.

The author(s) responsible for distribution of materials integral to the findings presented in this article in accordance with the policy described in the Instructions for Authors (www.plantphysiol.org) is: Jean-Benoit Charron (jean-benoit.charron@mcgill.ca).

B.F.M. and J.-B.C. designed the research; B.F.M. and A.B. performed the experiments and analyses; B.F.M., A.B., and J.-B.C. wrote the manuscript.

[OPEN]Articles can be viewed without a subscription.

www.plantphysiol.org/cgi/doi/10.1104/pp.19.01195

performance under cold (Thomashow, 1999). Cold acclimation is orchestrated by the expression of cold-regulated genes, notably through the C-repeat binding factor pathway (Thomashow, 1999). Despite the recognized importance of plant morphology in freezing tolerance, the interaction between cold acclimation and morphological development has not been thoroughly studied (Körner, 2016). Cold acclimation is the main mechanism by which plants increase their freezing tolerance. Studies define cold acclimation as early events of cold response (Bond et al., 2011). However, under cold conditions, both early and longer-term responses likely contribute to the establishment of a freezing-tolerant phenotype. Providing temperatures are not so cold as to completely inhibit growth, plant development and the morphology acquired under cold conditions may hence play a role in freezing tolerance (Equiza et al., 2001; Patel and Franklin, 2009).

While cold hardiness is important for surviving cold stress, plants also maximize their persistence in temperate climates by adjusting their phenology to seasonality (Chouard, 1960). The cold-mediated regulation of flowering time, often coupled to a longer photoperiod, ensures that flowering occurs when winter is over. Indeed, temperate plants usually require a relatively long exposure to cold temperatures to acquire the capacity to flower through a process known as vernalization (Chouard, 1960). In temperate cereals, vernalization is characterized by the activation of the MADS-box transcription factor *VERNALIZATION1* (*VRN1*) and the quantitative accumulation of its transcripts in response to cold (Danyluk et al., 2003). The activation of *VRN1* occurs in tandem with epigenetic changes on the *VRN1* gene, such as the depletion of histone 3 Lys 27 trimethylation (H3K27me3; Oliver et al., 2009, 2013; Woods et al., 2017). Because the activation of *VRN1* is maintained after exposure to cold, vernalization has been referred to as the "memory of winter."

Plants generally respond to colder temperatures and lower photoperiod during fall. These are thought to be important signals for cold acclimation and vernalization and could possibly induce structural change. Although these processes are triggered by similar signals, the connection between their regulations is not well known. Probably because cold acclimation and vernalization appear to occur independently in Arabidopsis (*Arabidopsis thaliana*; Bond et al., 2011), most research efforts that investigated their interaction focused on temperate cereals. Indeed, cold acclimation capacity and responsiveness to vernalization treatments appear to be linked in wheat (*Triticum aestivum*) and barley (*Hordeum vulgare*; Fowler et al., 1996; Dhillon et al., 2010). A negative correlation between the vernalized state and freezing tolerance has been reported as plants reaching vernalization saturation started to lose their freezing tolerance (Fowler et al., 1996). Furthermore, it was shown that vernalization requirement and cold acclimation capacity appear to be linked to alleles of *VRN1* in wheat (Ganeshan et al., 2008; Laudencia-Chingcuanco et al., 2011). *VRN1* has been proposed as a connective node between cold acclimation and vernalization (Dhillon et al., 2010). Studies have also highlighted the role of *VRN1* in regulating elements of plant phenotypic development (Preston and Kellogg, 2008; Voss-Fels et al., 2018). *VRN1* may hence play a fundamental role in cold adaptation in temperate cereals. Temperate cereal crops are complex systems to study the interaction between growth, cold acclimation, and vernalization because of the complex relationship between these traits and their inconvenient use in laboratory settings. Moreover, knowledge gained from studying these domesticated crops may not reflect the natural variation and the adaptive mechanisms potentially found in wild organisms. The undomesticated cereal model *Brachypodium distachyon* can thus be viewed as a useful candidate species to study cold adaptation and its regulation in a natural context.

The temperate grass *B. distachyon* is native to the Mediterranean region, where it grows as a spring or winter annual (Colton-Gagnon et al., 2014; Des Marais and Juenger, 2016). The species displays a range of vernalization requirements and has the capacity to cold acclimate (Colton-Gagnon et al., 2014; Ream et al., 2014; Ryu et al., 2014). Compared to wheat, however, *B. distachyon* has so far displayed a limited capacity to increase its tolerance to freezing upon cold acclimation. Unlike spring and winter wheat that can, for example, increase their tolerance to freezing by 6°C and 18°C, respectively (decrease in lethal temperature for 50% of the plants, LT_{50}; Ganeshan et al., 2008), *B. distachyon* accessions have shown a modest gain in freezing tolerance of 2°C regardless of their vernalization requirement (Colton-Gagnon et al., 2014). The limited capacity for acclimation of *B. distachyon* is particularly intriguing because this species has been shown to have an extensive natural variation in vernalization requirements. While it is possible that the species possesses a limited cold acclimation capacity, we hypothesized that the low-temperature treatments commonly used under controlled conditions are unsuccessful in eliciting the extent of the species' freezing tolerance. By developing a method to simulate seasonal change, we have attempted to further characterize the species' freezing-tolerant phenotype and highlighted a regulatory function for *VRN1* in cold acclimation and plant morphology in *B. distachyon*.

RESULTS

Diurnal Freezing Models the Transition from Summer to Winter in *B. distachyon*'s Natural Range

It was previously shown that when cold-acclimated for 28 d under a typical constant-chilling (CC) treatment (4°C), the freezing tolerance of *B. distachyon* is estimated at an LT_{50} of −10°C (Colton-Gagnon et al., 2014). This LT_{50} appears to be the maximal tolerance of this species when acclimated under constant chilling, as up to 49 d of cold acclimation under either short- or long-day

photoperiod does not further increase its freezing tolerance (Supplemental Fig. S1). However, substantially lower freezing temperatures were measured in *B. distachyon*'s natural range. These observations may indicate that in addition to inducing visible chilling stress, constant chilling might not reproduce the cues responsible for complete cold acclimation in *B. distachyon* (Supplemental Fig. S1). Therefore, we attempted to find a more appropriate experimental protocol to induce sturdier cold acclimation in the species and investigated the seasonal cues at geographically distinct locations in the species' natural range (represented by habitats H1 to H4). These locations correspond to the seed collection sites of four accessions of *B. distachyon*, from lowest to highest latitude: H1 in Iraq (Bd21-3), H2 in Spain (Bd30-1), H3 in Turkey (Bd18-1), and H4 in Ukraine (Bd29-1). The climatic conditions at these natural habitats H1 to H4 are, respectively, warm semiarid (Bsh), hot-summer Mediterranean (Csa), warm-summer Mediterranean/cold semiarid (Csb/Bsk), and humid subtropical/oceanic (Cfa/Cfb) according to the Köppen-Geiger classification system and may represent the extent of *B. distachyon*'s geographical range (Fig. 1; Supplemental Fig. S1).

Meteorological data reporting monthly averages of temperature (tmp), diurnal temperature range (dtr), frequency of frost days (frs), and photoperiod (pp) that span 1901 to 2017 was used to study seasonal change in the four locations. Principal component analysis was performed to highlight the difference in atmospheric conditions between seasons across the four habitats and between H1 and H4 (Fig. 1B). This analysis shows that the principal component1 appears to capture the seasonality shared among the habitats H1 to H4, while principal component2 describes differences between the conditions in habitats H1 to H4. It appears that seasons are clearly defined across the four habitats and that atmospheric conditions are more markedly different between seasons than between the selected habitats (Fig. 1B). Moreover, we plotted the monthly dtr over the monthly mean tmp at habitats H1 to H4 (Fig. 1C). These representations depict the temperature variations experienced in a typical day at each month in each habitat, based on 1901 to 2017 monthly average values. According to this data, *B. distachyon* experiences relatively high diurnal temperature variations that are highest during the summer (>20°C in H1) and lowest in winter (< 6°C in H4) with a yearly average of 11.25°C across habitats H1 to H4 (Fig. 1C; Supplemental Table S1).

To visualize the change in atmospheric conditions during the progression of seasons, we plotted the atmospheric variables monthly tmp, dtr, frs, and pp in a circular diagram (Fig. 1D). This diagram illustrates how seasons are characterized by gradual change in the atmospheric variables tmp, dtr, frs, and pp. The lowest monthly values are toward the center of the circle and the highest on the edge (Fig. 1D). Unsurprisingly, summers have highest tmp, dtr, and pp, while on the opposite, winters show highest frs and lowest tmp, dtr, and pp. Indeed, the transition from summer to winter sees gradual decreases first in photoperiod (pp), second in mean tmp, and third in dtr, while the frs increases during fall. In other words, photoperiod leads the change, followed by mean temperature, dtr, and frs.

In an attempt to unite the cues that signal summer-to-winter change, we have selected specific values of the seasonal atmospheric variables that are representative of (1) summer, (2) fall, and (3) winter. We combined the lowest photoperiod (end of fall) to a mean temperature typical of fall, a high dtr typical of summer, and a high frs typical of winter into a single treatment (called diurnal freezing [DF]; circled in Fig. 1, D and E). The DF treatment is characterized by cycles of 24 h that simulate winter-like nighttime frost with a minimum of −1°C and a maximum of 22°C during the day. This temperature range models a summer-like dtr and a fall-like mean tmp of 8.7°C. The DF treatment associates this temperature regime to a late fall-like photoperiod of 8 h of daily light (Fig. 1E; Supplemental Table S1).

Constant Chilling and DF Emulate Distinct Cold Conditions and Induce Divergent Responses in *B. distachyon*

To further characterize the progressively colder temperatures of the fall, we compared the naturally occurring chilling and freezing at *B. distachyon* habitats H1 to H4 and DF to constant chilling (CC), to a typical laboratory cold treatment. Hours and rates of chilling (between 0°C and 8°C) and freezing (temperature below 0°C) were determined using meteorological data collected every three hours by nearby meteorological stations (Supplemental Table S2). Both chilling and freezing events were observed at habitats H1, H2, H3, and H4 between September and March. In all habitats, the occurrence of freezing increases as the hours of chilling increase (Fig. 2). Also, both chilling and freezing rates increase with the progression of fall and peak at wintertime (Fig. 2C). Unsurprisingly, DF reproduces the relation between the occurrence of chilling and freezing, along with chilling and freezing rates that approximate the conditions in habitats H1 to H4 (Figs. 2, B and C). Conversely, the absence of freezing in CC, coupled to a chilling rate twice as high as the maximum natural chilling rate, clearly shows that the CC treatment does not reproduce the natural occurrence of cold in these habitats (Figs. 2, B and C).

To measure the growth response of *B. distachyon* to CC and DF, we measured the number tillers and leaf chlorophyll content in plants exposed to either treatment for 7 to 56 d. *B. distachyon* developed fewer tillers under CC than under DF. After 56 d of exposure to either treatment, DF plants tended to be more similar to plants growing under control conditions than plants growing under CC conditions (Fig. 2D). Moreover, all accessions lose more chlorophyll when exposed to CC than to DF (Fig. 2E). Notably, DF did not induce visible chilling stress injuries as observed under CC (Supplemental Fig. S1C). Hence, CC reproduces maximum chilling conditions that limit growth and reduce plant chlorophyll content. Conversely,

DF simulates conditions that are closer to natural events and leads to less growth reduction than CC.

DF Leads to Higher Freezing Tolerance

To compare the cold acclimation response under CC and DF, we measured the freezing tolerance, the transcript accumulation of cold-regulated (COR) genes, and the levels of nonstructural carbohydrates and proline (Pro) in plants exposed to either treatment. We measured survival to freezing temperatures of Bd21-3, Bd30-1, Bd18-1, and Bd29-1 subjected to CC or DF for 7 d by performing whole-plant freeze tests, during which plants were exposed to gradually lower freezing temperatures (Fig. 3). DF-treated plants showed measurably

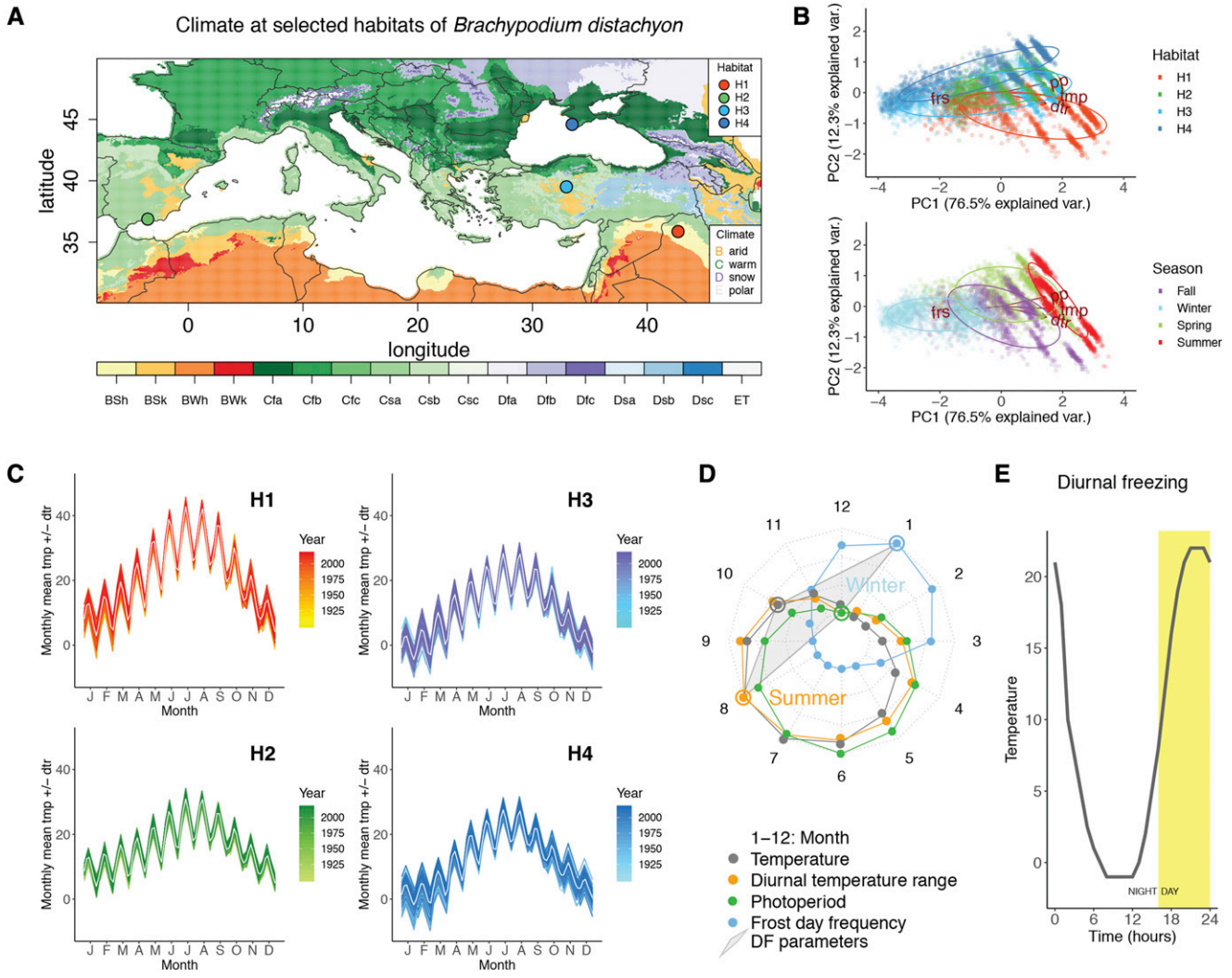

Figure 1. Specific seasonal cues observed at four habitats of *B. distachyon* can be combined into a diurnal freezing treatment to mimic seasonal change. A, Climate at selected geographical locations (habitats) that correspond to the parental seed collection sites of accessions Bd21-3 (H1), Bd30-1 (H2), Bd18-1 (H3), and Bd29-1 (H4). The colors correspond to the following climate: Group B, dry (arid) climates. BSh, hot semiarid; BSk, cold semiarid; BWh, hot desert; BWk, cold deser. Group C, temperate/mesothermal climates. Csa, Mediterranean hot summer; Csb, Mediterranean warm/cool summer; Csc, Mediterranean cold summer; Cfa, humid subtropical; Cfb, oceanic; Cfc, subpolar oceanic. Group D, continental/microthermal climates. Dfa, hot-summer humid continental; Dfb, warm-summer humid continental; Dfc, subarctic; Dsa, Mediterranean-influenced hot-summer humid continental; Dsb, Mediterranean-influenced warm-summer humid continental; Dsc, Mediterranean-influenced subarctic. Group E, polar climates. ET, tundra. B, Principal component analyses illustrating clusters of the climatic data by habitat H1 to H4 (top) or by season across the four habitats (bottom) over the following variables: tmp, dtr, pp, and frs. C, Diagram depicting a typical daily temperature variation for each month at each habitat. Values represent the monthly average diurnal temperature range centered around the monthly average temperature from data spanning 1901 to 2017 in H1 to H4. D, Radar plot summarizing the gradual monthly change of tmp, dtr, pp, and frs that characterize seasonal change and representative values (circled) selected as parameters of a diurnal freezing treatment (DF): frs observed in winter, dtr observed in summer, and values of tmp and pp observed in the fall. E, Representation of a 24-h cycle of DF.

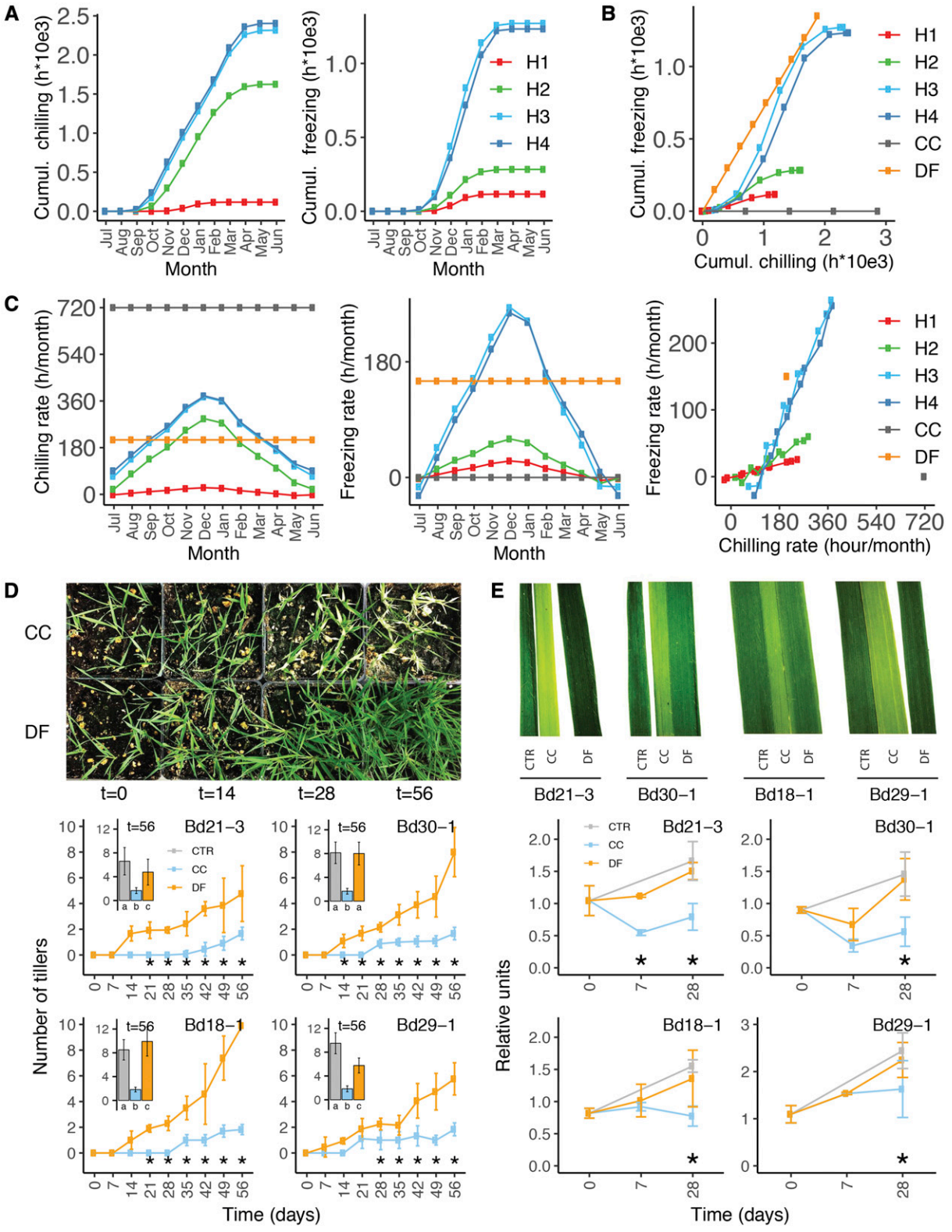

Figure 2. Constant chilling and diurnal freezing simulate distinct chilling and freezing conditions and induce divergent growth responses. A, Cumulative hours of chilling (between 0°C and 8°C) and freezing (< 0°C) in four habitats of *B. distachyon* H1 to H4 compared to CC and DF treatments. B, Cumulative freezing in relation to cumulative chilling in H1 to H4, CC, and DF. C, Actual rate of chilling and freezing in the four habitats based on meteorological stations from 1973 to 2017 (Supplemental Table S2) compared to CC and DF. D, Number of tillers in control (CTR), CC-, and DF-treated *B. distachyon* accessions Bd21-3, Bd30-1,

higher survival to freezing in all accessions. Moreover, we measured the survival of Bd21-3 CC28 and DF28 plants that were subjected to either treatment for 28 d. The results show that at −12°C, more than 60% of DF28 survive, compared to almost 0% of CC28 (Fig. 3B). Therefore, we estimated that the LT_{50} of DF28 plants (which we were not able to measure) is probably below −12°C.

Transcript accumulation of cold-regulated (*COR*) genes at the first 16 and 24 h of exposure to CC or DF suggests that cold acclimation occurs under both treatments. However, *COR* gene profiles are different between the two treatments, as illustrated by the early high levels of *ICE-RECRYSTALLIZATION INHIBITOR* (*IRI*) observed under DF (Fig. 3C). Interestingly, all accessions seem to respond similarly to either CC or DF. We further deepened our analysis by measuring the contents of Pro and nonstructural carbohydrates. Both treatments induced to similar levels the accumulation of raffinose, Glc, Fru, and high-density polymerization fructans (Fig. 3D). Nevertheless, the accumulation of Suc, whole-soluble sugars, starch, and total nonstructural carbohydrates were higher in CC-treated plants. Similarly, the accumulation of Pro was higher in CC-treated than in DF-treated plants (Fig. 3E). Altogether, CC and DF induce distinct cold acclimation in *B. distachyon*. DF-treated plants gain a higher freezing tolerance but accumulate lower levels of total nonstructural carbohydrates and Pro compared to CC-treated plants.

CC and DF Induce Contrasting Vernalization and Flowering Responses

To determine the effects of DF on flowering time, we measured the number of days to heading in Bd21-3 (facultative accession with a low vernalization requirement) and Bd18-1 (winter accession with high vernalization requirement) that were vernalized under CC, a typical vernalization treatment, or DF. Plants were vernalized under either treatment for 7 to 56 d prior to being transferred to a flowering-inducing treatment (long-day conditions). Compared to nonvernalized controls, both cold treatments decreased time to flowering in Bd21-3 and Bd18-1. Although both treatments induced flowering, when vernalized for up to 21 d, CC-treated Bd21-3 flowered earlier than DF-treated Bd21-3. Similarly, CC-treated Bd18-1 vernalized for 7 and 14 d also flowered earlier than DF-treated Bd18-1. However, the flowering time of CC-treated and DF-treated plants in all later time points were equivalent (Fig. 4). Hence, vernalization under DF could effectively induce a flowering response in both *B. distachyon* accessions but did so slightly slower than the CC treatment.

We further measured the transcript levels of the cold-responsive vernalization gene *VERNALIZATION1* (*VRN1*), whose expression is known to provide flowering competence in *B. distachyon*. *VRN1* transcripts accumulate to higher levels in CC than in DF in all four accessions tested (Fig. 4B). Linear regression of form $y = mx+b$ showed that, according to the m coefficient in CC- and DF-fitted models, *VRN1* transcript levels accumulate ~5.8 times faster under CC than under DF (Fig. 4B). Plotting the levels of *VRN1* transcripts against the corresponding days to heading in the vernalization-requiring accession Bd18-1 shows that DF-treated plants reach minimum flowering time with lower *VRN1* transcript levels than in CC-treated plants (Supplemental Fig. S2). Again, as CC and DF induce similar flowering responses, linear regression shows that the accumulation of *VRN1* transcripts under DF induces vernalization, with ~5.6 lower *VRN1* transcript levels than under CC (Supplemental Fig. S2). Hence, plants exposed to DF show a vernalization response that leads to flowering competence with significantly lower *VRN1* transcript levels, which indicates that lower expression of VRN1 than previously observed under CC are necessary to reach flowering competence in *B. distachyon*. Moreover, the vernalization response under DF also suggests the influence of DF-responsive factors on vernalization and flowering.

The vernalization response is characterized by the activation of *VRN1* that sees its chromatin transition from a closed to an open state under cold exposure. Thus, we measured the levels of histone H3, repressive histone mark H3K27me3, and polymerase-II-bound DNA at the *VRN1* locus on nonvernalized (NV) control (56-week-old plants grown under short-day 22°C) and vernalized CC56 (CC) and DF56 (DF) Bd21-3 plants. NV show the highest levels of H3 and H3K27me3 and no binding of polymerase II at the *VRN1* locus (Fig. 4C). CC leads to significantly lower H3 and H3K27me3 levels and significantly higher signals of polymerase II binding to *VRN1* compared to both NV and DF. Compared to NV, DF shows lower nucleosome density levels around the first exon of *VRN1* (*CaRG* and *R1*) and lower H3K27me3 levels toward the end of the first intron (*R6*), indicating a vernalization response. However, the overall chromatin state of *VRN1* observed in DF-vernalized plants appears to be similar to NV rather than CC vernalized. Therefore, the chromatin state of *VRN1* measured under DF suggests a moderate vernalization response compared to the highly relaxed state and the highly active transcription measured under CC.

Because CC and DF induced a similar flowering response and contrasting epigenetic and transcriptional

Figure 2. (*Continued.*)
Bd18-1, and Bd29-1 for 7 to 56 d. E, Relative total chlorophyll contents in CTR, CC, and DF measured in Bd21-3, Bd30-1, Bd18-1, and Bd29-1 at 0, 7, and 28 d. * indicates statistical differences between CC and DF; $P < 0.05$; error bars represent SD between three biological replicates.

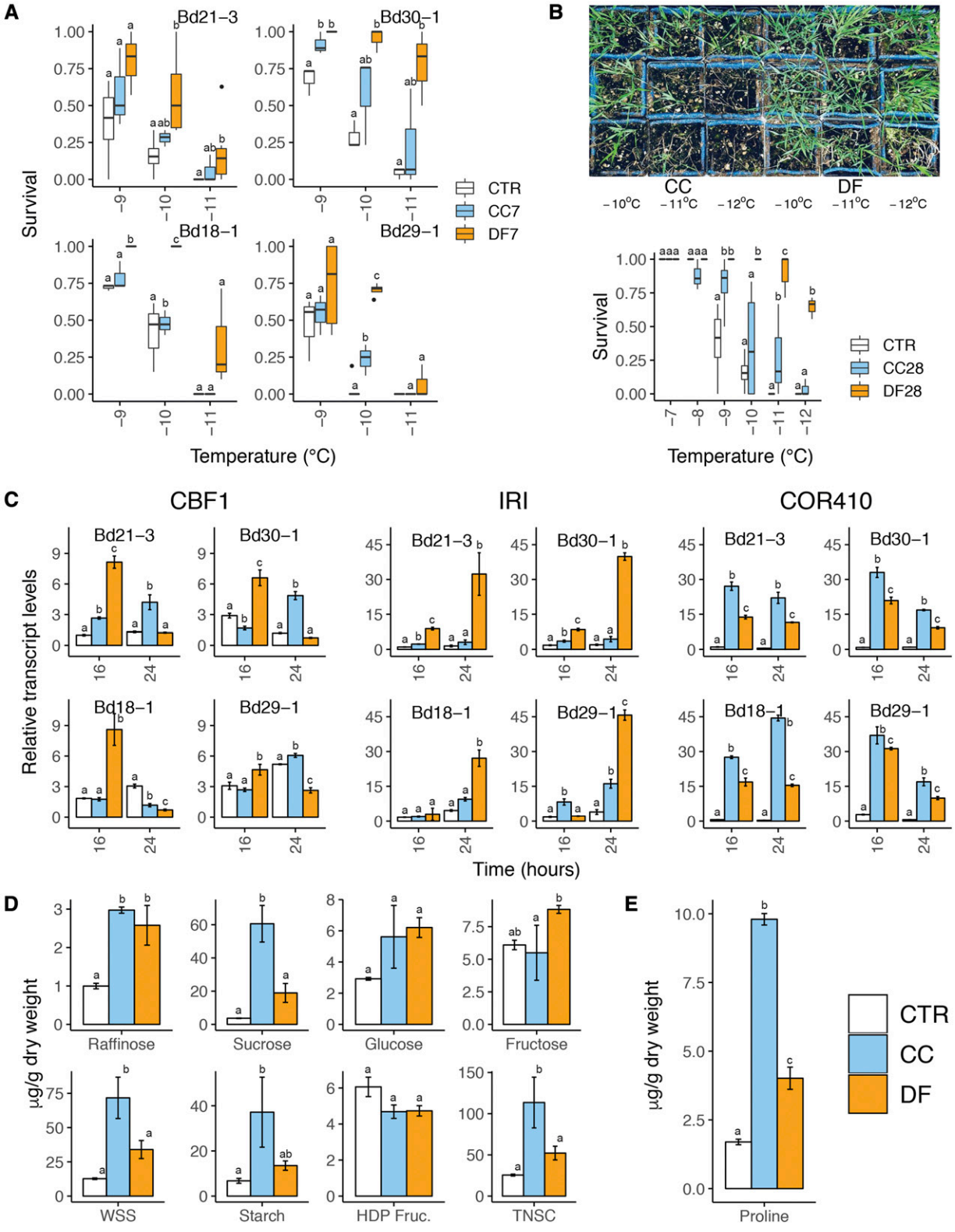

Figure 3. Constant chilling and diurnal freezing induce contrasting cold acclimation and freezing tolerance. A, Survival to freezing in Bd21-3, Bd30-1, Bd18-1, and Bd29-1 after 7 d in either control conditions (CTR; short-day 22°C), constant chilling (CC), or diurnal freezing (DF) measured in whole-plant freeze tests in which temperature hourly decreases by 1°C down to −12°C. B, Survival to freezing in Bd21-3 after 28 d in either control (CTR), constant chilling (CC), or diurnal freezing (DF). C, Relative transcript accumulation of *C-REPEAT BINDING FACTOR 1* (*CBF1*), *ICE-RECRISTALLIZATION INHIBITOR* (IRI), and

state of *VRN1*, we measured the expression of FLOWERING LOCUS T (FT), whose expression promotes flowering, as previously identified in *B. distachyon* (Ream et al., 2014). Prior to the transfer to flower-inducing conditions, transcript levels of *FT* are higher in plants vernalized under CC compared to plants vernalized under DF (Fig. 4D). However, when transferred to flowering conditions, plants vernalized under DF accumulate *FT* transcripts to significantly higher levels than CC-vernalized plants despite lower VRN1 levels (Fig. 4E). Hence, change in *FT* may occur independently of *VRN1* expression under DF. To determine the effects of *VRN1* expression and the acquisition of flowering competence under CC and DF, we measured the transcript levels of *VRN1* and *FT* in previously described *VRN1* overexpressor (UBI:*VRN1*) and knockdown (ami*VRN1*) lines that respectively display rapid flowering without vernalization and strong flowering delay when vernalized in response to CC and DF (Ream et al., 2014; Woods et al., 2016). As expected, UBI:*VRN1* shows higher transcript levels of *VRN1* under both cold treatments (Supplemental Fig. S3). As observed with Bd21-3 (Fig. 4E), both *VRN1* transgenic lines that were vernalized under DF show higher transcript levels of *FT* once transferred to flowering conditions, compared to CC-vernalized plants (Supplemental Fig. S3). Therefore, these results suggest that CC and DF induce different vernalization and flowering responses and that vernalization under DF appears to lead to a higher expression of *FT* independently of the expression of *VRN1*.

High *VRN1* Transcript Levels Limit Cold Acclimation and Freezing Tolerance

Plants grown under CC accumulate high levels of *VRN1* transcripts and display a moderate tolerance to freezing. Conversely, plants grown under DF develop a high tolerance to freezing with lower levels of *VRN1*. Hence, we investigated the link between *VRN1* expression, cold acclimation, and freezing tolerance in *VRN1* overexpressor (UBI:*VRN1*) and knockdown (ami*VRN1*) transgenic lines. With a similar non-acclimated freezing tolerance and a lower cold-acclimated freezing tolerance, UBI:*VRN1* showed a lower capacity to cold-acclimate under both CC and DF compared to 10A and ami:*VRN1* plants in whole-plant freeze test (Fig. 5A). Within the first 16 h of exposure to DF, the profiles of *COR* gene transcript accumulation in the *VRN1* transgenic lines suggest that VRN1 influences *COR* gene transcription (Fig. 5B). Although *VRN1* transgenics show complex differences in the transcription profiles of *COR* genes, the transcript levels of the cold-responsive transcription factors *C-REPEAT BINDING FACTOR1* (*CBF1*), *CBF2*, and *BCF3* were significantly different between all lines at 4 and 16 h for CBF1, at 16 h for CBF2, and at 12 h for CBF3; UBI:*VRN1* showed the lowest while ami*VRN1* showed the highest transcript levels (Fig. 5B). In addition to being significantly different from one another, both transgenic lines also showed lower transcript levels compared to the control line 10A for the structural *COR* gene *COR410* at 12 and 16 h.

To determine whether the VRN1 protein was directly interfering with the transcriptional regulation of *CBF* genes, we performed a chromatin immunoprecipitation-quantitative PCR (ChIP-qPCR) assay on the ACV5-tagged VRN1 fusion protein in the UBI:*VRN1* background (Fig. 5C). The results suggest that VRN1 binds to the promoters of *CBF1* and *CBF3* and hence that high VRN1 levels affect cold acclimation by interacting with *CBF*'s promoters.

VRN1 Influences Plant Morphology and Winter Hardiness

As the DF treatment is closer to natural conditions, studying how the growth, cold acclimation, and vernalization responses are integrated under this treatment may better explain winter hardiness in *B. distachyon*. Indeed, DF-treated plants developed a distinctive plant structure. We recorded final height, final leaf number, number of tillers, number of spikes, dry weight, and weight of seeds in control, CC-, and DF-treated Bd21-3 and Bd18-1. CC56 and DF56 were both shorter than control CTR56 and tend to produce more spikes and heavier seeds (Fig. 6A). However, CC and DF led to two distinct plant morphologies with large differences in the number of final leaves and tillers. Indeed, DF-treated plants developed compact plant structure with a high number of leaves and tillers and consequently tended to produce more biomass (Fig. 6A). In addition to producing more leaves and tillers than CC-treated plants, DF plants acquired a compact structure compared to control plants, with similar numbers of tillers. Indeed, the length between each node (where tillers emerge) is significantly smaller in DF plants (Supplemental Fig. S4). This structure appears to better insulate the crown tissues of the plant, which are believed to be an important structure for surviving freezing (Supplemental Fig. S4).

Phenotypic measurements along with the corresponding *VRN1* transcript levels (Fig. 4A) and days to heading (Fig. 4B) in CC7-56 and DF7-56 of both Bd21-3 and Bd18-1 were summarized in a heatmap. Associated dendrograms show that CC35-56 followed by CC21-28

Figure 3. (*Continued.*)
COLD-REGULATED410 (*COR410*) at 16 or 24 h after exposure to CC or DF. D, Nonstructural carbohydrate contents in CTR, CC-, and DF-treated plants after 7 d in either treatment. E, Pro contents in CTR, CC-, and DF-treated plants after 7 d in either treatment. Error bars represent SD among three biological replicates; different letters represent statistically significant differences; $P < 0.05$.

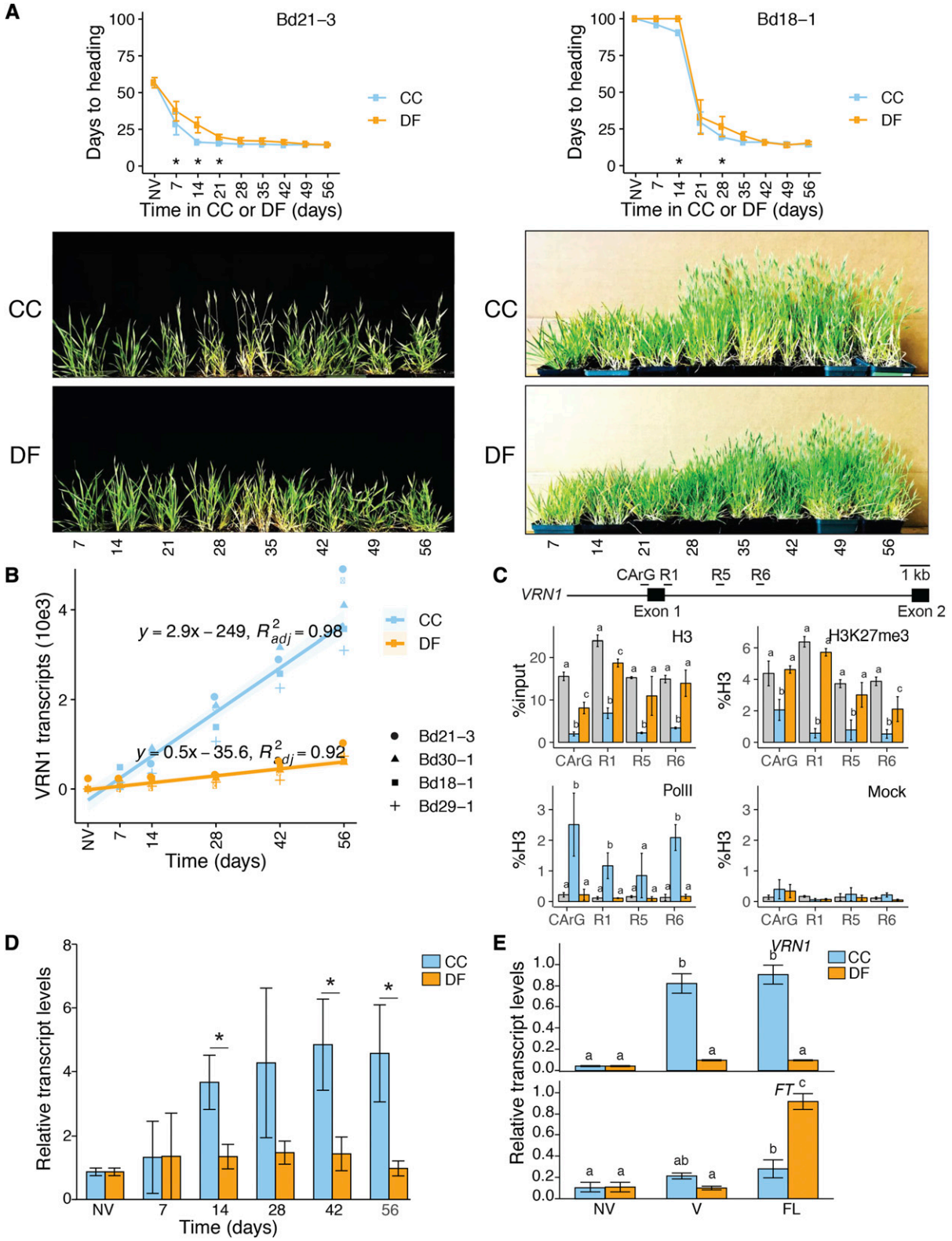

Figure 4. CC and DF lead to flowering competence but induce contrasting vernalization and flowering responses. A, Days to heading in weak vernalization requiring Bd21-3 and strong vernalization requiring Bd18-1. Prior to being transferred to flower inducing conditions, plants were either nonvernalized (NV; grown under noninductive control conditions) or vernalized for 7 to 56 d (7-56) under CC or DF. B, Relative levels of *VRN1* transcripts in Bd21-3, Bd30-1, Bd18-1, and Bd29-1 in a nonvernalizing or vernalization treatment CC or DF for 7 to 56 d. Linear regression of the form $y = mx+b$ was fitted on both CC- and DF-induced

form distinct phenotypic groups, highlighting the effects of long-term CC on plant phenotype. In contrast, DF-treated plants cluster together along with CTR0, CTR56, and CC7-14. Generally, the number of final leaves decreases over time under both CC and DF until vernalization saturation. However, only DF plants showed a subsequent increase in final leaf number (Fig. 6B; Supplemental Fig. S5). In addition, the heatmap shows that *VRN1* is an important discriminating factor between CC- and DF-treated plants. As CC and DF lead to disparate plant morphologies and drastically different transcription of *VRN1*, we investigated the effects of high *VRN1* expression on plant morphology.

B. distachyon is a long-day plant that does not flower under 8 h light/day (e.g. control SD22°C, CC, and DF). Hence, when grown for 56 d under noninductive photoperiod, UBI:*VRN1* plants adopted a distinct plant stature compared to control and ami*VRN1* plants (Fig. 6C). UBI:*VRN1* were taller and displayed fewer tillers under all treatments. Moreover, UBI:*VRN1* DF56 plants that have flowered had around twice the height and half the number of tillers and leaves compared to 10A (empty-vector control) and ami:*VRN1* plants (Supplemental Fig. S6). When grown under DF, *ami:VRN1* plants adopt a shorter stature than control plants (Fig. 6C). These results show that *VRN1* expression influences plant morphology. Possibly, the phenotypic difference between CC-treated and DF-treated plants can be at least partly attributed to the levels of *VRN1* transcripts, as also suggested by the dendrogram (Fig. 4B): high levels prevent the development of short-statured plants with high numbers of tillers and leaves. Importantly, UBI:*VRN1* failed to produce a compact plant structure under DF. These results allowed us to generate a model of the effects of *VRN1*'s expression on vernalization, plant phenotype, and winter hardiness (Fig. 6D).

DISCUSSION

DF Induces High Freezing Tolerance in *B. distachyon*

The DF treatment was designed to maximize the signals of seasonal change toward winter by combining specific values of seasonal atmospheric variables that are typical of summer, fall, and winter in four habitats inside the natural range of *B. distachyon*. Compared to CC, the DF treatment induced higher freezing tolerance in all tested accessions. The transcript accumulation profiles of *COR* genes, as well as the levels of Pro and nonstructural carbohydrates, indicate that DF induces a different cold acclimation response compared to the one elicited by CC. Cold acclimation induced by freezing temperatures has been described in temperate cereals, *Brassica napus*, and Arabidopsis (Kacperska and Kulesza, 1987; Herman et al., 2006; Takahashi et al., 2019). This response, termed subzero acclimation or described as a secondary stage of cold acclimation, appears to regroup acclimation mechanisms different from those of chilling-induced acclimation. Plants exposed to transient nondamaging frost and diurnally freezing temperatures were shown to undergo changes in photosynthesis, organelle structure, phospholipid content and composition, cell wall composition, and water potential that contribute to increasing freezing tolerance (Andrews et al., 1974; Sikorska and Kacperska-Palacz, 1979; Kacperska and Kulesza, 1987; Le et al., 2008; Takahashi et al., 2019). Hence, by exposing plants to negative temperatures, DF likely induces cold acclimation mechanisms different from those induced by CC.

Under DF, *B. distachyon* developed similarly to control conditions but acquired more leaves and a more compact plant stature (Fig. 6, A and B). This compact plant stature contributes to insulating the crown tissues (Supplemental Fig. S4) and was described as a morphological adaptation to cold climates in alpine plants (Körner, 2016). This more extensive growth response compared to CC can in part be attributed to the promotion of leaf initiation by warmer temperatures (Li et al., 2019). Moreover, it was also shown that subzero acclimation can affect plant growth capability and that variations in the excitation state of PSII caused by day/night temperature changes can affect growth and plant structure (Kacperska and Kulesza, 1987; Gray et al., 1997). As such, the compact plant stature displayed by DF-treated plants could hypothetically be the result of individual or a combination of environmental factors, such as freezing, warm temperatures, and diurnal temperature variation and likely contributed to the significantly higher freezing tolerance measured in DF28 compared to CC28.

Because the daily temperature cycles are relatively wide in *B. distachyon*'s natural range, the occurrence of freezing and chilling appear to be closer to the freeze-thaw cycles of DF than to stable chilling temperatures (Figs. 1C and 2, A–C–C). This particularity simultaneously allows the occurrence of cold and subzero acclimation, coupled to a morphological response. Hence, the response induced by DF may elicit mechanisms of cold acclimation and freezing tolerance closer to what

Figure 4. (*Continued.*)
VRN1 transcript levels (*y*) over time under either treatment (*x*). C, Chromatin state of the *VRN1* gene in Bd21-3 at 56 d of exposure to CC or DF; levels of H3, H3K27me3, levels of polymerase II (Pol II) binding, and mock control at four regions of *VRN1* (regions adapted from Woods et al. [2017]). D, Relative levels of *FT* transcripts in Bd21-3 NV or vernalized for 7 to 56 d (7-56) under CC or DF. E, Relative transcript levels of *VRN1* in Bd21-3 and of the flowering gene *FT* in NV control, CC56, or DF56 (vernalized; V), or a week after being transferred to flower inducing conditions (flowering; FL) after vernalization. Error bars (B–E) represent SD between three biological replicates; different letters and asterisks represent statistically significant differences; $P < 0.05$.

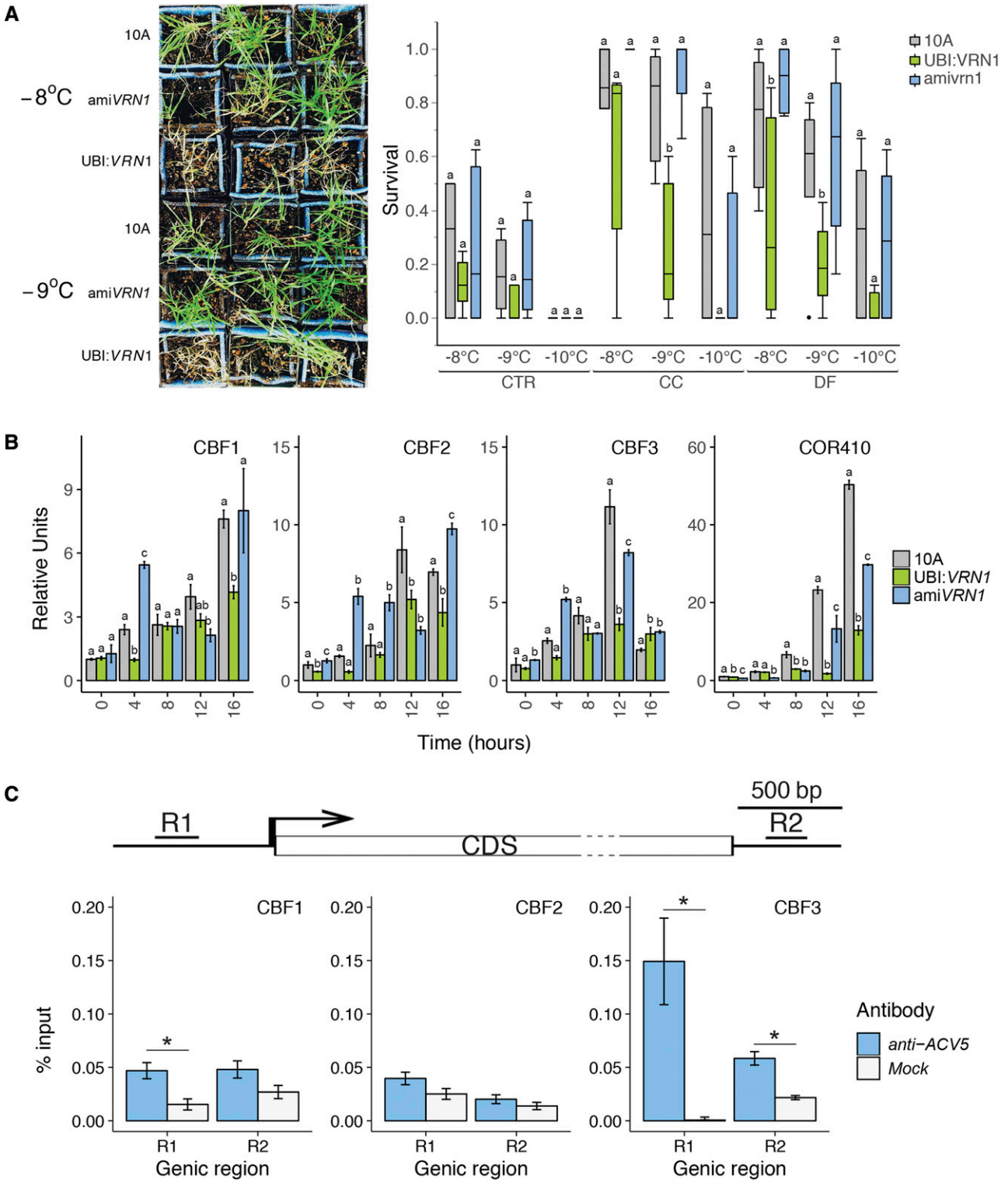

Figure 5. High *VRN1* expression limits cold acclimation and freezing tolerance. A, Survival to freezing measured of empty-vector pANIC 10A control (10A), *VRN1* overexpressor (UBI:*VRN1*), and *VRN1* knockdown (ami*VRN1*) lines grown under control (CTR) and cold-acclimated under CC or DF. B, Relative levels of cold acclimation gene transcripts at 0, 4, 8, 12, and 16 h under DF. C, Chromatin immunoprecipitation showing binding of the ACV5-tagged VRN1 protein in UBI:*VRN1* background on cold-responsive transcription factors *CBF1*, *CBF2*, and *CBF3*. Error bars represent SD between three biological replicates. Different letters and asterisks represent statistically significant differences; $P < 0.05$.

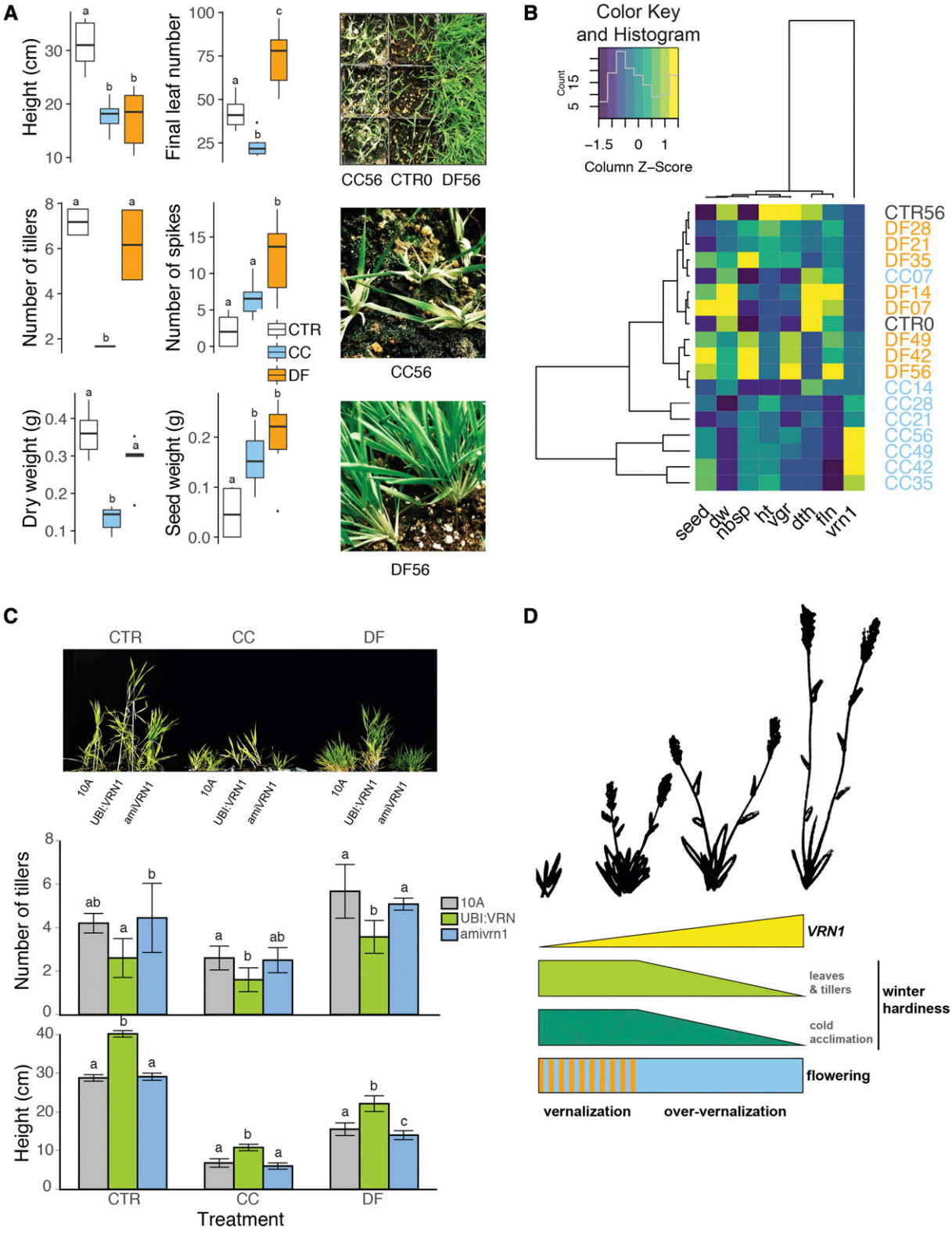

Figure 6. The development of a winter-hardy phenotype is mediated by the expression levels of *VRN1*. A, Phenotypic data on control (CTR56), CC, and DF plants exposed for 56 d to either treatment (CC56 and DF56) in Bd21-3 and Bd18-1. Pictures illustrating the contrast between CTR0 (equivalent to CC0 and DF0), CC56, and DF56 plant phenotypes (*B. distachyon* Bd30-1). Error bars represent SD between six biological replicates; different letters represent statistically significant differences; $P < 0.05$. B, Heatmap and dendrogram summarizing these differences in phenotype in CC- or DF-treated Bd21-3 and Bd18-1 (CC7-56,

the species undergoes in a natural context. Although a range of vernalization responsiveness was found in *B. distachyon*, studies so far show that all accessions underwent vernalization when exposed to cold (Ream et al., 2014), and because they all showed the capacity to increase their freezing tolerance, no "true" spring accession was found in the species (Colton-Gagnon et al., 2014). Because *B. distachyon* can grow under cold conditions, acquiring an adaptive morphology to mitigate the negative effects of freezing during cold exposure may hence be part of its freezing tolerance strategy.

High VRN1 Expression Inhibits Freezing Tolerance

The results show that high expression of *VRN1* limits cold acclimation and the acquisition of a compact plant stature. Our results show that *VRN1* overexpressors have a limited ability to cold acclimate and tolerate freezing and show lower freezing tolerance and lower *COR* gene expression (Fig. 5, A and B). This observation can be at least partly explained by the direct binding of the *VRN1* protein to the *CBF1* and *CBF3* promoters. As *B. distachyon* is an obligate long-day plant, light conditions under control, CC, and DF treatments (8 h light per day) did not induce flowering. Under noninductive treatments (SD, CC, and DF), *VRN1* overexpressors grew into taller plants with fewer tillers and leaves, and *VRN1* knockdown plants had a shorter stature under DF but showed a similar number of tillers and leaves. As the *VRN1* overexpressors failed to develop a freezing-tolerant plant structure normally induced by DF (Fig. 6C), *VRN1* seems to be involved in cold acclimation and the regulation of plant morphology, with high *VRN1* expression inhibiting freezing tolerance in *B. distachyon*. Interestingly, previous work on barley demonstrated that VRN1 binds and regulates the expression of diverse target genes, such as genes involved in hormone metabolism and *CBF* (Deng et al., 2015). In addition to regulating vernalization in cereals, *VRN1* is active in wheat meristems during flower morphogenesis (Preston and Kellogg, 2008). Furthermore, recent work demonstrated that *VRN1* influences root architecture in barley and wheat (Voss-Fels et al., 2018). Our results suggest that Bd*VRN1* plays a basic role in cold adaptation by regulating vernalization, cold acclimation, and plant morphology. This finding is in accordance with putative functions of *VRN1* reported in this species and other temperate cereals (Dhillon et al., 2010; Feng et al., 2017). Recent work suggested that vernalization, in that case associated with high *VRN1* expression, limits freezing tolerance in *B. distachyon* (Feng et al., 2017). Our results indicate that vernalization can occur with relatively low expression of *VRN1* and hence can coincide with high freezing tolerance, as illustrated by DF-treated plants. Our findings support that *VRN1* is involved in cold acclimation and plant development, and as such, its expression levels are determinant in acquiring a freezing-tolerant phenotype.

DF Induces a Distinct Vernalization and Flowering Response

CC and DF induced distinct responses characterized by markedly different *VRN1* levels. CC-treated plants showed a lower tolerance to freezing and higher *VRN1* expression levels compared to DF-treated plants. According to the function of *VRN1* in regulating the freezing-tolerant phenotype, the higher expression levels measured under CC are likely involved in limiting freezing tolerance but unsurprisingly have induced a strong vernalization response. Under both treatments, vernalization is characterized by the activation of *VRN1* and the associated epigenetic changes (lower nucleosome density and depletion in H3K27me3) that were previously observed in *B. distachyon* and in barley (Oliver et al., 2013; Woods et al., 2017). However, CC-induced vernalization showed higher *VRN1* expression that extended long after vernalization saturation (when plants had fully transitioned to flowering competence). This highly active transcriptional state was linked to the presence of RNA polymerase II and few nucleosomes on the *VRN1* locus, indicating an extensively relaxed chromatin state. Conversely, the lower transcript levels of *VRN1* measured under DF coincided with higher nucleosome and H3K27me3 levels compared to CC and was overall closer to the NV chromatin state of *VRN1*. Interestingly, CC-vernalized and DF-vernalized plants flowered at relatively the same time but had contrasting levels of both *VRN1* and the flowering gene *FT* under cold treatment, but also under flowering conditions postvernalization (Fig. 4, D and E). Vernalization under DF induced lower *FT* expression but led to higher *FT* expression once transitioned to a flowering treatment. This change in *FT* expression occurred independently of *VRN1* expression levels, as also shown in *VRN1* transgenic lines (Supplemental Fig. S3). It was previously shown that *FT* overexpression *B. distachyon* lines also flower rapidly without vernalization (Ream et al., 2014). Hence, strictly speaking, the higher expression of

Figure 6. (*Continued.*)
DF7-56, CTR0, and CTR56). vrn1, *VRN1* transcript levels; vgr, number of tillers; ht, height; dth, days to heading; fln, final leaf number; nbsp, number of spikes; dw, dry weight; seed, total seed weight. (C) Morphology of empty-vector pANIC 10A control (10A), *VRN1* overexpressor (UBI:*VRN1*), and *VRN1* knockdown (ami*VRN1*) lines grown in control (CTR56; short-day 22°C), constant chilling (CC56), and diurnal freezing (DF56; no flowering occurs under these treatments). Error bars represent SD between biological replicates; different letters represent statistically significant differences; $P < 0.05$. D, Model summarizing the relationship between *VRN1* expression levels, flowering, and winter hardiness.

FT in DF-vernalized plants once transitioned to flowering could compensate for the lower *VRN1* levels induced by DF. Studies have shown that there is a regulatory loop between *VRN1* and *FT*, as high transcript levels of *FT* were measured in UBI:*VRN1* and high levels of *VRN1* were measured in *FT*-overexpressing mutants (Ream et al., 2014). The DF treatment seems to induce the expression of *FT* postvernalization independently of this regulatory loop, which suggests the existence of different flowering mechanisms than previously described. Overall, these results show that vernalization and the acquisition of flowering competence can occur with a relatively weaker activation of *VRN1* expression than previously described (Colton-Gagnon et al., 2014).

DF Is an Artificial Treatment That Elicits Seemingly More Balanced Cold Responses

Cold induces acclimation during early exposure and leads to both physiological and morphological changes that can contribute to maximizing survival to freezing. Vernalization becomes relevant when flowering can occur, thus in later stages (probably at springtime, when photoperiod increases in the case of *B. distachyon*). Therefore, it seems logical that cold-induced reproductive growth would occur subsequently and without inhibiting the development of freezing tolerance. CC and DF treatment lead to two different outcomes regarding the unfolding of cold acclimation, plant growth, vernalization, and flowering in *B. distachyon*. On the one hand, DF treatment resulted in cold-acclimated, short-statured, and flowering-competent plants. On the other hand, CC treatment resulted in highly vernalized plants that displayed lower cold acclimation and signs of chilling stress. Therefore, the response induced by DF appears to be more effective in inducing freezing tolerance and flowering. Because DF more closely models the natural onset of cold, this manifestation of cold acclimation and vernalization may better reflect the plants' cold-adaptive traits. Nevertheless, the DF treatment is artificial and the responses it elicits may diverge from the plant's natural cold responses. The DF treatment is a representational approach to reproduce and combine extreme natural cues of a given geographical range. The combination of extreme signals like the co-occurrence of low photoperiod with repetitive freezing and high dtr are not typically experienced by plants. However, this unique combination may have exacerbated some of the responses associated with seasonal change, such as the existence of morphological mechanisms of freezing tolerance and an alternative induction of vernalization and flowering. Hence, the DF treatment appears to have experimental value. Other crucial factors such as water availability, light quality, and light intensity were maintained constant in our study and would deserve more attention in such treatments, especially as drought appears to have applied an important selective pressure on the species (Des Marais and Juenger, 2016). It is of course impossible to reproduce the complexity of nature indoors; however, our study shows that attempting to simulate natural conditions of plant's native range can lead to new and informative observations. Bridging the gap between basic experimental research and field studies is a crucial step in making relevant conclusions about the relationship between natural phenomena and biology, especially when investigating the consequences of anthropogenic climate change. Altogether, the approach presented in this study can contribute to the understanding of the effect of natural environmental conditions and could be applied to other plant species with different climatic specificities. Importantly, the DF treatment contributed to revealing a basic function for *VRN1* in cold adaptation. The regulation of its expression levels appears to be central to an adaptive unfolding of cold acclimation and morphological change that increase freezing tolerance. As studies have shown, the implication of *VRN1* in regulating cold adaptation makes this gene a prime subject to understand the regulation and the evolution of cold adaptation in plants, as previously suggested (McKeown et al., 2016).

CC Induces Chilling Stress and Suboptimal Cold Acclimation

Although CC has been a useful treatment in the discovery and study of cold responses in many species, it does not seem to reproduce the natural patterns of cold acclimation conditions present in the native range of *B. distachyon* and appears to induce chilling damages along with limited cold acclimation in the species. It has already been proposed that the lack of progress in effectively improving winter hardiness in plants is partly due to a failure to reproduce in laboratory settings the complexity of natural conditions (Gusta and Wisniewski, 2013). We observed larger accumulation of total nonstructural carbohydrates and Pro in response to CC than to DF (Fig. 3). The lower levels of nonstructural carbohydrates measured in DF plants may be linked to a different allocation, for example toward biomass (Fig. 6). Even though the accumulation of Pro is considered as a marker of cold acclimation in many species, it does not correlate with freezing tolerance in *B. distachyon* (Colton-Gagnon et al., 2014). In fact, Pro is known to accumulate in plants during stress (Hayat et al., 2012), and the higher Pro concentrations measured under CC may hence be a sign of stress (Supplemental Fig. S1). Overall, it seems that the levels of Pro and nonstructural carbohydrates reflect the different responses induced by CC and DF rather than indicating cold acclimation and the levels of freezing tolerance.

CC Vernalization Leads to Oververnalization

This study suggests that previous observations of negative correlations between cold acclimation and the vernalized state in temperate cereals may have been

biased by high expression of *VRN1* induced by the traditional use of CC to study cold acclimation and vernalization under controlled conditions. For many years, the number of leaves at senescence (final leaf number) has been used as an indicator of the number of days to heading or of the transition between the vegetative to the reproductive stage (Wang et al., 1995). Here, the relationship between days to heading and final leaf number is visible in early time points in both CC- and DF-vernalized plants (Supplemental Fig. S5). However, plants exposed to DF begin to reaccumulate leaves after vernalization saturation (i.e. 28 d in Fig. 6A; Supplemental Fig. S5). Thus, as also observed in *VRN1* overexpressors, the number of leaves appears to be mostly indicative of high expression of *VRN1*, rather than the vernalized state (Fig. 6C; Supplemental Fig. S6). From these observations, we can suggest two stages during DF-induced vernalization: (1) acquisition of flowering competence and (2) development after vernalization saturation. Probably because the expression of *VRN1* is relatively low throughout vernalization under DF, its effects on the number of leaves and tillers is attenuated once vernalization saturation is reached (Supplemental Fig. S5). Therefore, the acquisition of flowering competence would be a "checkpoint" event during the development of *B. distachyon*, rather than a developmental determinant. As vernalization saturation is reached under DF, *B. distachyon* can resume its vegetative growth and, subsequently, once flowering signals are present (e.g. higher temperatures and long days), can transition to reproductive growth by upregulating *FT* (Fig. 4E; Supplemental Fig. S3). As such, the unfolding of development and the acquisition of flowering competence could be linked to the expression of *VRN1* during vernalization and flowering to the expression of *FT* postvernalization. A tentative model summarizes the influence of *VRN1* on winter hardiness and flowering in Figure 6D.

CC-induced vernalization is characterized by high expression of *VRN1* and *FT* (Fig. 4) and prompt flowering with no change in *VRN1* or *FT* expression, as seen in wild-type and *VRN1* overexpressing and knockdown transgenic plants. Therefore, CC appears to prime plants differently to flowering than DF. It was previously described that overly long exposure to cold induces growth-inhibitory effects in monocots. This phenomenon, termed oververnalization, is attributed to delayed development and reduced numbers of buds, leaves, and spikes (Weiler and Langhans, 1968; Derera and Ellison, 1974). Notably, the number of leaves and tillers are lower in *VRN1* overexpressors (Fig. 6C; Supplemental Fig. S6). CC-induced vernalization also leads to fewer tillers, leaves, and spikes, which may be linked to the growth inhibition imposed by the treatment and to the high expression of *VRN1*. If we consider plant stature, growth, and tillering as factors that influence winter hardiness in *B. distachyon*, the growth inhibition and *VRN1* overexpression induced by CC inhibit winter survival. As the overly high *VRN1* expression may not be required to achieve flowering and negatively affects freezing tolerance, it appears that the oververnalization induced by CC is therefore ultimately deleterious to winter hardiness. Because CC is far from modeling the atmospheric conditions measured in *B. distachyon*'s natural range, this state of oververnalization may hence deviate substantially from what can be observed in natural populations of *B. distachyon*.

Conclusion

This study reports an innovative approach to model atmospheric cues of seasonal change. By combining cues specific of summer, fall, and winter, the DF treatment induced cold acclimation and morphological change toward a freezing-tolerant plant structure and led to flowering competence through an expression of *VRN1* significantly lower than previously described. The results show that high expression of *VRN1* inhibits freezing tolerance and that CC treatments induce artificial responses that limit freezing tolerance in *B. distachyon*. The work presented in this study also suggests that *VRN1* plays a fundamental role in cold adaptation by regulating flowering, cold acclimation, and morphological development. By providing a glimpse of how cold adaptation responses are integrated in *B. distachyon*, this study shows that modeling elements of the natural context in laboratory experiments can provide new perspectives to scientific knowledge.

MATERIALS AND METHODS

Climatic and Meteorological Datasets

Monthly average data for tmp, dtr, and frs were retrieved from the Climatic Research Unit TS4.01 dataset (Harris et al., 2014) covering data from 1901 to 2017 at stated or estimated collection sites of the parent accessions of *Brachypodium distachyon* inbred lines Bd21-3, Bd30-1, Bd18-1, and Bd29-1 corresponding to four habitats named H1, H2, H3, and H4, respectively. The data were retrieved by GPS coordinates from datasets archived by the Centre for Environmental Data Analysis (University of East Anglia Climatic Research Unit et al., 2017). Climates at the four habitats, as well as the data used to generate the map displayed in Figure 1A, were obtained from a Köppen-Geiger climate world map that was reanalyzed in 2017, and produced with data from 1986 to 2010 (Kottek et al., 2006). Hourly temperature data used to generate Figures 1C and 2, A–C, and Supplemental Figure S1B were retrieved from the HadISD: Global subdaily, surface meteorological station data, 1931–2017, v2.0.2.2017f (Dunn et al., 2015; Met Office Hadley Centre and National Centers for Environmental Information – NOAA, 2018) for specific stations as summarized in Supplemental Table S2. The data and raster file of the climate map were analyzed in R to produce Figure 1A (R Core Team, 2013).

Plant Growth and Treatments

B. distachyon inbred lines Bd21-3, Bd30-1, Bd18-1, and Bd29-1 seeds were soaked for 2 h and stratified at 4°C in the dark for 7 d. Stratified seeds were planted 3 × 3 in 3-inch 0.5-L pots filled with 160 g of G2 Agromix (Fafard et Frères), which were placed in an environmental growth chamber (Conviron) at 22°C under photosynthetically active radiation intensity of 150 μmol m^{-2} s^{-1} for 8 h of light per day. When plants reach the three-leaf stage (~14 d under control conditions), they were either transferred to the CC treatment at 4°C in an environmental growth chamber or to the DF treatment (see details in Supplemental Table S1) programmed into a LT-36VL growth chamber (Percival

Scientific). CC and DF light conditions were identical to control (8 h of light per day at 150 μmol m^{-2} s^{-1}), and all plants were kept equally watered throughout the treatments. To induce flowering, plants were transferred to 16 h of light per day also at a photosynthetically active radiation intensity of 150 μmol m^{-2} s^{-1} on a growth bench at 25°C and maintained watered until senescence.

Phenotypic Measurements

Days to heading were determined from the date plants were moved to flower-inducing conditions to the date when plants showed first visible emergence of heads (flowers). The number of tillers and plant height were determined prior to being transferred to flowering conditions except when mentioned otherwise. Total chlorophyll was extracted using methanol from fresh and ground pooled leaf tissue of three plants and observed by spectrophotometry as previously described (Ritchie, 2006). Final leaf number, number of spikes, dry weight, and seed weight were determined after senescence. Dry weight measurements were performed on total aerial tissue (without seeds) after thorough drying of plant tissues.

Survival to Freezing

Plant survival to freezing was measured in whole-plant freeze tests in a LT-36VL growth chamber (Percival Scientific). The freezing program decreases the chamber temperature from −1°C to −12°C at the rate of 1°C per h. Prior to the freeze test, the pots were watered to soil saturation and randomly placed in the growth chamber. Three randomly selected pots containing nine plants each were removed after each hourly plateau from −7°C to −12°C. The plants were then left to thaw at 4°C in the dark for 24 h, then switched to 22°C with no light for an additional 24 h before being moved back to control conditions. Percent survival was determined after a week of recovery under control conditions. Prior to planting, all pots contained insulating pads to prevent drastic soil freezing and emulate natural soil cooling conditions. Plants exposed to whole-plant freeze test were at the three-leaf stage in all experiments except for CC28 and DF28 plants that had a higher number of tillers.

Pro and Sugar Quantification

Tissue used for Pro and sugar quantification were pooled aerial tissue from 27 plants per replicate and dehydrated, extracted, and quantified as previously described (Colton-Gagnon et al., 2014).

RNA Extraction and Reverse Transcription (RT)-qPCR

Plant tissue was sampled from whole aerial tissue of plants at the three-leaf stage for cold acclimation samples (Fig. 2D) and 1 g of leaf tissue for vernalization samples (Fig. 3, B and C). Sampled tissue was flash-frozen in liquid nitrogen before storage at −80°C. Each sampling was performed by pooling plant tissue from three plants. Samples were then extracted using EZ-10 spin column plant RNA miniprep kit (cat. no. BS82314, Bio Basic) following the manufacturer's protocol. Reverse-transcriptase cDNA was synthesized using iScript advanced cDNA synthesis kit for RT-qPCR (cat. no. 1725037, Bio-Rad) as stated in the manufacturer's protocol. Relative transcript levels were determined by RT-qPCR reactions with Green-2-Go qPCR mastermix (cat. no. QPCR004, Bio Basic) using a CFX Connect Real Time system (Bio-Rad) and relative transcript levels were analyzed following the ΔΔCT method using *UBC18* gene as reference on biologically independent replicates (Hong et al., 2008; Ream et al., 2014; Woods et al., 2017). The genes studied were previously identified as important cold-responsive genes in *B. distachyon* and include *CBF1*, *CBF2*, *CBF3* (Colton-Gagnon et al., 2014; Ryu et al., 2014), *IRI* (Herman et al., 2006; Colton-Gagnon et al., 2014; Bredow et al., 2016), and *VRN1* (Colton-Gagnon et al., 2014; Ream et al., 2014). Primer sequences can be found in Supplemental Table S3.

VRN1 Transgenic Lines

VRN1 mutant lines UBI:*VRN1* and ami:*VRN1* were previously described and published (Ream et al., 2014; Woods et al., 2016).

ChIP and qPCR

ChIP was performed from a pool of three plants' cross linked aerial tissue. ChIP was performed with anti-histone H3 antibody (cat. no. ab1791, Abcam), anti-histone H3 antibody (tri-methyl K27; cat. no. ab6002, Abcam), and anti-RNA polymerase II antibody (clone CTD4H8, Sigma-Aldrich) performed on the VRN1 locus. For the VRN1 protein binding analysis, ChIP was performed using anti-ACV5 antibody (cat. no. A2980, Sigma-Aldrich) targeted to the VRN1-ACV5 fusion protein expressed by UBI:*VRN1* plants and a mock no-antibody control. Immunoprecipitated samples were analyzed by qPCR using the reagents described above for RT-qPCR and expressed by percent input (H3) or percent H3 as previously described (Mayer et al., 2015) without removing the mock signal from IP signals. Primer sequences can be found in Supplemental Table S3.

Statistical Analysis

One-way ANOVA tests followed by Tukey's test were performed in JMP (SAS Institute; https://www.jmp.com/en_ca/home.html). Statistical significance was determined with $P < 0.05$ on at least three independent biological replicates, including fold values for qPCR data. Error bars represent SD between biological replicates. Linear model fits were performed in R using *lm()* for Figure 4, B and C.

Accession Numbers

Sequence data from this article can be found in the GenBank/EMBL data libraries under the following accession numbers: *UBC18* (Bradi4g00660), *VRN1* (Bradi1g08340), *CBF1* (Bradi3g51630), *CBF2* (Bradi1g49560), *CBF3* (Bradi4g35650), *IRI* (Bradi5g27350), *COR410* (Bradi3g51200), and *FT* (Bradi1g48830).

Supplemental Data

The following supplemental materials are available.

Supplemental Figure S1. Freezing tolerance in CC-treated *B. distachyon* and associated chilling stress.

Supplemental Figure S2. *VRN1* transcript levels in relation to days to heading in CC- and DF-treated vernalization requiring Bd18-1.

Supplemental Figure S3. Expression of VRN1 and FT in NV, vernalized in CC and DF, and flowering postvernalization VRN1 transgenic lines.

Supplemental Figure S4. The compact plant structure produced by DF may better insulate crown tissues.

Supplemental Figure S5. Phenotype of Bd21-3 and Bd18-1 in response to CC and DF at 7 to 56 d of exposure.

Supplemental Figure S6. Phenotype of DF56 *VRN1* transgenic plants at senescence.

Supplemental Table S1. Summary of the dataset on habitats H1 to H4 and the DF treatment and the detailed temperature and light cycles of DF.

Supplemental Table S2. Accessions selected for this study, the corresponding geographic location of their parental seed collection site, and associated climate.

Supplemental Table S3. Primers used in this study.

ACKNOWLEDGMENTS

The authors are thankful to Daniel Woods and Richard Amasino for providing the transgenic lines used in this study.

Received September 27, 2019; accepted November 29, 2019; published December 16, 2019.

LITERATURE CITED

Andrews CJ, Pomeroy MK, de la Roche IA (1974) Influence of light and diurnal freezing temperature on the cold hardiness of winter wheat seedlings. Can J Bot **52:** 2539–2546

Bond DM, Dennis ES, Finnegan EJ (2011) The low temperature response pathways for cold acclimation and vernalization are independent. Plant Cell Environ **34:** 1737–1748

Bredow M, Vanderbeld B, Walker VK (2016) Knockdown of ice-binding proteins in *Brachypodium distachyon* demonstrates their role in freeze protection. PLoS One **11:** e0167941

Chouard P (1960) Vernalization and its relations to dormancy. Annu Rev Plant Physiol **11:** 191–238

Colton-Gagnon K, Ali-Benali MA, Mayer BF, Dionne R, Bertrand A, Do Carmo S, Charron JB (2014) Comparative analysis of the cold acclimation and freezing tolerance capacities of seven diploid *Brachypodium distachyon* accessions. Ann Bot **113:** 681–693

Danyluk J, Kane NA, Breton G, Limin AE, Fowler DB, Sarhan F (2003) TaVRT-1, a putative transcription factor associated with vegetative to reproductive transition in cereals. Plant Physiol **132:** 1849–1860

Deng W, Casao MC, Wang P, Sato K, Hayes PM, Finnegan EJ, Trevaskis B (2015) Direct links between the vernalization response and other key traits of cereal crops. Nat Commun **6:** 5882

Derera NF, Ellison FW (1974) The response of some wheat cultivars to extended vernalization. Cereal Res Comm **2:** 159–166

Des Marais DL, Juenger TE (2016) Brachypodium and the abiotic environment. *In* JP Vogel, ed, Genetics and Genomics of Brachypodium. Springer International Publishing, Cham, Switzerland, pp 291–311

Dhillon T, Pearce SP, Stockinger EJ, Distelfeld A, Li C, Knox AK, Vashegyi I, Vágújfalvi A, Galiba G, Dubcovsky J (2010) Regulation of freezing tolerance and flowering in temperate cereals: the VRN-1 connection. Plant Physiol **153:** 1846–1858

Dunn RJH, Willett KM, Parker DE, Mitchell L (2015) Expanding HadISD: Quality-controlled, sub-daily station data from 1931. Clim Past Discuss **11:** 4569–4600

Equiza MA, Miravé JP, Tognetti JA (2001) Morphological, anatomical and physiological responses related to differential shoot vs. root growth inhibition at low temperature in spring and winter wheat. Ann Bot **87:** 67–76

Feng Y, Yin Y, Fei S (2017) *BdVRN1* expression confers flowering competency and is negatively correlated with freezing tolerance in *Brachypodium distachyon*. Front Plant Sci **8:** 1107

Fowler DB, Limin AE, Wang S-Y, Ward RW (1996) Relationship between low-temperature tolerance and vernalization response in wheat and rye. Can J Plant Sci **76:** 37–42

Ganeshan S, Vitamvas P, Fowler DB, Chibbar RN (2008) Quantitative expression analysis of selected COR genes reveals their differential expression in leaf and crown tissues of wheat (*Triticum aestivum* L.) during an extended low temperature acclimation regimen. J Exp Bot **59:** 2393–2402

Gray GR, Chauvin LP, Sarhan F, Huner N (1997) Cold acclimation and freezing tolerance (a complex interaction of light and temperature). Plant Physiol **114:** 467–474

Gusta LV, Wisniewski M (2013) Understanding plant cold hardiness: An opinion. Physiol Plant **147:** 4–14

Harris I, Jones PD, Osborn TJ, Lister DH (2014) Updated high-resolution grids of monthly climatic observations – the CRU TS3.10 dataset. Int J Climatol **34:** 623–642

Harris IC, Jones PD; University of East Anglia Climatic Research Unit (2017) CRU TS4.01: Climatic Research Unit (CRU) Time-Series (TS) version 4.01 of high-resolution gridded data of month-by-month variation in climate (Jan. 1901-Dec. 2016). Centre for Environmental Data Analysis. Available at: http://dx.doi.org/10.5285/58a8802721c94c66ae45c3baa4d814d0

Hayat S, Hayat Q, Alyemeni MN, Wani AS, Pichtel J, Ahmad A (2012) Role of proline under changing environments: A review. Plant Signal Behav **7:** 1456–1466

Herman EM, Rotter K, Premakumar R, Elwinger G, Bae H, Ehler-King L, Chen S, Livingston DP III (2006) Additional freeze hardiness in wheat acquired by exposure to -3 degreesC is associated with extensive physiological, morphological, and molecular changes. J Exp Bot **57:** 3601–3618

Hong SY, Seo PJ, Yang MS, Xiang F, Park CM (2008) Exploring valid reference genes for gene expression studies in *Brachypodium distachyon* by real-time PCR. BMC Plant Biol **8:** 112

Kacperska A, Kulesza L (1987) Frost resistance of winter rape leaves as related to the changes in water potential and growth capability. Physiol Plant **71:** 483–488

Körner C (2016) Plant adaptation to cold climates. F1000Res **5:** 2769

Kottek M, Grieser J, Beck C, Rudolf B, Rubel F (2006) World map of the Koppen-Geiger climate classification updated. Meteorol Z **15:** 259–263

Laudencia-Chingcuanco D, Ganeshan S, You F, Fowler B, Chibbar R, Anderson O (2011) Genome-wide gene expression analysis supports a developmental model of low temperature tolerance gene regulation in wheat (*Triticum aestivum* L.). BMC Genomics **12:** 299

Le MQ, Engelsberger WR, Hincha DK (2008) Natural genetic variation in acclimation capacity at sub-zero temperatures after cold acclimation at 4°C in different Arabidopsis thaliana accessions. Cryobiology **57:** 104–112

Li M, Kennedy A, Huybrechts M, Dochy N, Geuten K (2019) The effect of ambient temperature on *Brachypodium distachyon* development. Front Plant Sci **10:** 1011

Mayer BF, Ali-Benali MA, Demone J, Bertrand A, Charron JB (2015) Cold acclimation induces distinctive changes in the chromatin state and transcript levels of COR genes in *Cannabis sativa* varieties with contrasting cold acclimation capacities. Physiol Plant **155:** 281–295

McKeown M, Schubert M, Marcussen T, Fjellheim S, Preston JC (2016) Evidence for an early origin of vernalization responsiveness in temperate Pooideae grasses. Plant Physiol **172:** 416–426

Met Office Hadley Centre, National Centers for Environmental Information - NOAA (2018) HadISD: Global sub-daily, surface meteorological station data, 1931-2017, v2.0.2.2017f. Centre for Environmental Data Analysis. http://dx.doi.org/10.5285/acee665e3e664a73b8ad247e99b343d5

Oliver SN, Deng W, Casao MC, Trevaskis B (2013) Low temperatures induce rapid changes in chromatin state and transcript levels of the cereal VERNALIZATION1 gene. J Exp Bot **64:** 2413–2422

Oliver SN, Finnegan EJ, Dennis ES, Peacock WJ, Trevaskis B (2009) Vernalization-induced flowering in cereals is associated with changes in histone methylation at the VERNALIZATION1 gene. Proc Natl Acad Sci USA **106:** 8386–8391

Patel D, Franklin KA (2009) Temperature-regulation of plant architecture. Plant Signal Behav **4:** 577–579

Preston JC, Kellogg EA (2008) Discrete developmental roles for temperate cereal grass VERNALIZATION1/FRUITFULL-like genes in flowering competency and the transition to flowering. Plant Physiol **146:** 265–276

R Core Team (2013) R: A Language and Environment for Statistical Computing. R Foundation for Statistical Computing, Vienna, Austria

Ream TS, Woods DP, Schwartz CJ, Sanabria CP, Mahoy JA, Walters EM, Kaeppler HF, Amasino RM (2014) Interaction of photoperiod and vernalization determines flowering time of *Brachypodium distachyon*. Plant Physiol **164:** 694–709

Ritchie RJ (2006) Consistent sets of spectrophotometric chlorophyll equations for acetone, methanol and ethanol solvents. Photosynth Res **89:** 27–41

Ryu JY, Hong SY, Jo SH, Woo JC, Lee S, Park CM (2014) Molecular and functional characterization of cold-responsive C-repeat binding factors from *Brachypodium distachyon*. BMC Plant Biol **14:** 15

Sikorska E, Kacperska-Palacz A (1979) Phospholipid involvement in frost tolerance. Physiol Plant **47:** 144–150

Takahashi D, Gorka M, Erban A, Graf A, Kopka J, Zuther E, Hincha DK (2019) Both cold and sub-zero acclimation induce cell wall modification and changes in the extracellular proteome in *Arabidopsis thaliana*. Sci Rep **9:** 2289

Thomashow MF (1999) Plant cold acclimation: Freezing tolerance genes and regulatory mechanisms. Annu Rev Plant Physiol Plant Mol Biol **50:** 571–599

USGCRP (2017) **DJ Wuebbles, DW Fahey, KA Hibbard, DJ Dokken, BC Stewart, TK Maycock**, eds, Climate science special report: Fourth national climate assessment, Volume 1. U.S. Global Change Research Program, Washington, DC, 10.7930/J0J964J6

Voss-Fels KP, Robinson H, Mudge SR, Richard C, Newman S, Wittkop B, Stahl A, Friedt W, Frisch M, Gabur I, et al (2018) VERNALIZATION1 modulates root system architecture in wheat and barley. Mol Plant **11:** 226–229

Wang S-Y, Ward RW, Ritchie JT, Fischer RA, Schulthess U (1995) Vernalization in wheat I. A model based on the interchangeability of plant age and vernalization duration. Field Crops Res **41:** 91–100

Weiler T, Langhans RW (1968) Determination of vernalizing temperatures in vernalization requirements of *Lilium longiflorum* (Thunb.) cv. 'Ace'. Proc Am Soc Hortic Sci **93:** 623–629

Woods DP, McKeown MA, Dong Y, Preston JC, Amasino RM (2016) Evolution of VRN2/Ghd7-like genes in vernalization-mediated repression of grass flowering. Plant Physiol **170:** 2124–2135

Woods DP, Ream TS, Bouché F, Lee J, Thrower N, Wilkerson C, Amasino RM (2017) Establishment of a vernalization requirement in *Brachypodium distachyon* requires *REPRESSOR OF VERNALIZATION1*. Proc Natl Acad Sci USA **114:** 6623–6628